



1 **High efficiency of livestock ammonia emission controls on alleviating**
2 **particulate nitrate during a severe winter haze episode in northern China**

3
4 **Zhenying Xu¹, Mingxu Liu¹, Yu Song^{1*}, Shuxiao Wang^{2*}, Lin Zhang³, Tingting Xu¹,**
5 **Tiantian Wang¹, Caiqing Yan¹, Tian Zhou¹, Yele Sun⁴, Yuepeng Pan⁴, Min Hu¹, Mei**
6 **Zheng^{1*} and Tong Zhu¹**

7 ¹State Key Joint Laboratory of Environmental Simulation and Pollution Control,
8 Department of Environmental Science, Peking University, Beijing, 100871, China

9 ²State Key Joint Laboratory of Environment Simulation and Pollution Control, School of
10 Environment, Tsinghua University, Beijing 100084, China

11 ³Laboratory for Climate and Ocean-Atmosphere Studies, Department of Atmospheric and
12 Oceanic Sciences, School of Physics, Peking University, Beijing 100871, China

13 ⁴State Key Laboratory of Atmospheric Boundary Layer Physics and Atmospheric
14 Chemistry, Institute of Atmospheric Physics, Chinese Academy of Sciences, Beijing
15 100029, China

16 *Corresponding author: Yu Song (songyu@pku.edu.cn), Shuxiao Wang
17 (shxwang@tsinghua.edu.cn), Mei Zheng (mzheng@pku.edu.cn).

18

19

20

21

22

23

24

25

26

27

28

29

30

31



32 Abstract

33 Although nitrogen oxide (NO_x) emission controls have been implemented for several
34 years in northern China, recent observations show particulate nitrate (NO₃⁻) is becoming
35 increasingly important during haze episodes. In this study, we find that particulate NO₃⁻
36 formation would easily become NH₃-limited under severe haze conditions, enhancing its
37 sensitivity to NH₃ emission controls. Furthermore, improved manure management of
38 livestock husbandry could reduce 40% of NH₃ emissions (currently 100 kiloton per a
39 month) in winter of northern China. Under this emission reductions scenario, simulations
40 from the thermodynamic equilibrium model (ISORROPIA-II) and the Weather Research
41 and Forecast model coupled chemistry (WRF-Chem) all show that particulate NO₃⁻ could
42 be reduced by approximately 40% during a typical severe haze episode (averagely from
43 40.8 to 25.7 μg/m³). Our results indicate that reducing livestock NH₃ emissions would be
44 highly effective to reduce particulate NO₃⁻ during severe winter haze events.

45

46 1 Introduction

47 In northern China (including Beijing, Tianjin, Hebei, Shandong, Shanxi and Henan),
48 severe haze pollution events occur frequently during wintertime, with the concentration of
49 PM_{2.5} (particles with an aerodynamic diameter less than 2.5 μm) reaching hundreds of
50 micrograms per cubic meter (Wang et al., 2015;Zheng et al., 2015;Elser et al., 2016). In
51 severe haze events, secondary inorganic aerosol (SIA) plays a crucial role in haze formation,
52 accounting for 30–77% of PM_{2.5} (Huang et al., 2014). In October 2014, four extreme haze
53 episodes were reported in North China Plain (NCP), with the concentrations of PM_{2.5}
54 exceeding 400 μg/m³, and the concentrations of SNA (sulfate, nitrate, and ammonium) and
55 particulate nitrate (NO₃⁻) at this time exceeding 190 and 90 μg/m, respectively(Yang et al.,
56 2015).

57 To mitigate severe fine particle pollution, the Chinese government has been taking
58 strong measures to control SO₂ and NO_x emissions. It has been reported that SO₂ emissions
59 in China have been reduced by 75% since 2007 (Li et al., 2017a). Meanwhile, particulate
60 sulfate has also been found to decrease since 2005 (Geng et al., 2017). Liu et al. (2017a)
61 found that NO_x emissions in 48 Chinese cities decreased by 21% from 2011 to 2015.
62 Unfortunately, in recent years, no obvious decreasing trend in the concentration of
63 particulate NO₃⁻ had been observed in northern China (Zhang et al., 2015;Li et al., 2017b)
64 and the ratio of ammonium nitrate (NH₄NO₃) to SNA increased continuously during severe
65 haze events (Li et al., 2017d;Yang et al., 2017).

66 It was reported in recent studies that the large atmospheric NH₃ emissions in northern
67 China have made particulate NO₃⁻ become more important, and it will reduce the
68 effectiveness of existing PM_{2.5} control strategies through SO₂ and NO_x emission reductions
69 (Wang et al., 2013;Fu et al., 2017). However, the effectiveness of controlling NH₃
70 emissions in reducing particulate NO₃⁻ during severe winter haze events has not been
71 reported.

72 In this study, we firstly compile a comprehensive NH₃ emission inventory for northern
73 China in winter of 2015, and estimate the NH₃ emission reductions by improving manure
74 management. Then, the ISORROPIA-II and WRF-Chem models are used to investigate the



75 effectiveness of NH₃ emission reductions on alleviating particulate NO₃⁻ during a severe
76 haze episode. Finally, the molar ratio of observational data is used to explore the particulate
77 NO₃⁻ reductions efficiency during the wintertime.

78

79 2 Methods and Materials

80 2.1 Observational data

81 Hourly time-resolution aerosol and gas measurements were conducted at the Peking
82 University urban atmosphere environment monitoring station (PKUERS) (39.991N,
83 116.313E) in Beijing in December 2015 and December 2016. A commercialized semi-
84 continuous In-situ Gas and Aerosol Composition (IGAC) Monitor was used to measure the
85 concentrations of water-soluble ions (e.g., NH₄⁺, SO₄²⁻, NO₃⁻, Na⁺, K⁺, Ca²⁺, Mg²⁺, Cl⁻) in
86 PM_{2.5} and inorganic gases (e.g., NH₃, HNO₃, HCl). Relative humidity (RH) and
87 temperature were observed at 1-min resolution at the same site. The quality assurance and
88 control for the IGAC was described in Liu et al. (2017b). A typical severe haze episode
89 occurred during the 6 to 10 in December 2015, with daily average concentrations of PM_{2.5}
90 exceeding 150 µg/m³ for three days (PM_{2.5} data are from China National Environmental
91 Monitoring Centre). The average RH and temperature in this haze event were 60.9 ± 11.4%
92 and 276.5 ± 1.4 K. The south wind was dominant with wind speed mostly less than 3 m/s.
93 The average concentrations of particulate NO₃⁻, NH₄⁺ and SO₄²⁻ were 39.8 ± 14.7 µg/m³,
94 27.7 ± 8.6 µg/m³ and 42.4 ± 16.0 µg/m³, respectively. The ratios of particulate NO₃⁻
95 concentrations to SNA were 36.5 ± 4.0%.

96 2.2 NH₃ emission inventory

97 A comprehensive NH₃ emission inventory in 2015 at a monthly and 1 km × 1 km
98 resolution is developed based our previous studies (Huang et al., 2012;Kang et al., 2016).
99 A diverse range of sources, including both agricultural (livestock manure and chemical
100 fertilizer) and non-agricultural sectors (e.g., traffic, biomass burning etc.) were fully
101 considered. Recent studies documented that our results agreed well with the satellite
102 measurements by Infrared Atmospheric Sounding Interferometer (IASI) (Van Damme et
103 al., 2014) and Tropospheric Emission Spectrometer (TES), and inverse model results by
104 using ammonium (NH₄⁺) wet deposition data (Paulot et al., 2014;Zhang et al., 2018).
105 According to our inventory, the estimated NH₃ emission amount in northern China was 100
106 kiloton in December 2015. The largest source was livestock waste (57.0% of the total
107 emissions), following by vehicle (12.2%), chemical industry (8.8%), biomass burning
108 (5.4%), waste disposal (4.0%), synthetic fertilizer applications (2.4%) and other minor
109 sources (9.1%). The proportion of chemical fertilizer is very small due to the limited
110 fertilization activity in winter.

111 2.3 ISORROPIA-II and WRF-Chem models

112 The thermodynamic equilibrium model, ISORROPIA-II (Fountoukis and Nenes,
113 2007), being used to determine the phase state and composition of an NH₄⁺- SO₄²⁻- NO₃⁻-
114 K⁺- Ca²⁺- Mg²⁺- Na⁺- Cl⁻- H₂O aerosol system with its corresponding gas components
115 in thermodynamic equilibrium, was used to investigate the response of particulate NO₃⁻ to
116 NH₃ emission reductions. Using measurements of water-soluble ions, T and RH from
117 PKUERS as inputs, ISORROPIA-II can avoid the inherent uncertainty in estimates of



118 emission inventories, pollutant transport, and chemical transformation. In this study,
119 ISORROPIA-II was run in the “forward mode” and assuming particles are “metastable”
120 with no solid precipitates, which is due to the relatively high RH range observed during
121 this haze event ($RH = 60.9 \pm 11.4\%$).

122 We assess the performance of ISORROPIA-II by comparing measured and predicted
123 particulate NO_3^- , NH_4^+ and gaseous HNO_3 , NH_3 . An error metric, the mean bias (MB), is
124 used to quantify the bias (the description of MB is shown below Figure S1). The predicted
125 particulate NO_3^- , NH_4^+ and NH_3 agree well with the measurements and the value of R^2 are
126 0.99, 0.94 and 0.84, respectively (Figure S1). The MB is only $1.0 \pm 1.1 \mu\text{g}/\text{m}^3$, 0.3 ± 1.3
127 $\mu\text{g}/\text{m}^3$ and $-1.8 \pm 1.6 \mu\text{g}/\text{m}^3$, respectively. However, the model performs poorly on HNO_3 ,
128 with an R^2 of only 0.06 and a MB of $-1.0 \pm 1.1 \mu\text{g}/\text{m}^3$. This is because particulate NO_3^- is
129 predominantly in the particle phase (the mass ratio of particulate NO_3^- to the total nitric
130 acid ($\text{TN} = \text{NO}_3^- + \text{HNO}_3$) was $99.2 \pm 1.9\%$), small errors in predicting particulate NO_3^-
131 are amplified in HNO_3 predicting. Since the MB of HNO_3 is much smaller than the
132 observed particulate NO_3^- ($39.8 \pm 14.7 \mu\text{g}/\text{m}^3$) and NH_4^+ ($27.7 \pm 8.6 \mu\text{g}/\text{m}^3$), this bias have
133 little influence on simulating the efficiency of particulate NO_3^- reductions.

134 In the real atmosphere, changes in the level of total ammonia ($\text{TA} = \text{NH}_4^+ + \text{NH}_3$) can
135 affect the lifetime of TN (Pandis and Seinfeld, 1990). This is because the gaseous HNO_3
136 has a faster deposition rate in the atmosphere than particulate NO_3^- , and reductions in NH_4^+
137 may prompt particulate NO_3^- partitioning into the gas phase. In such a case, the
138 concentration of TN would not remain constant but decrease. In order to consider these,
139 we use the Weather Research and Forecast Model coupled Chemistry (WRF-Chem) model
140 (ver. 3.6.1) to investigate the effect of NH_3 emission controls on particulate NO_3^- formation
141 in the regional scale. The simulations were performed for the severe haze event during 6 to
142 10 December 2015. The modeling domain covered the whole northern China with
143 horizontal resolution of 25 km and 24 vertical layers from surface to 50 hPa. The initial
144 meteorological fields and boundary conditions were taken from the 6 h National Centers
145 for Environmental Prediction (NCEP) global final analysis with a $1^\circ \times 1^\circ$ spatial resolution.
146 The inorganic gas-aerosol equilibrium was predicted by Multicomponent Equilibrium
147 Solver for Aerosols (MESA) in WRF-Chem (Zaveri et al., 2005; Zaveri et al., 2008). The
148 Carbon-Bond Mechanism version Z (CBMZ) photochemical mechanism and Model for
149 Simulating Aerosol Interactions and Chemistry (MOSAIC) aerosol model were used in this
150 study (Fast et al., 2006). Anthropogenic emissions from power plants, industrial sites,
151 residential locations, and vehicles were taken from the Multi-resolution Emission
152 Inventory for China (MEIC; available at www.meicmodel.org). The WRF-Chem model
153 could approximately reproduce the temporal variations of inorganic aerosol components in
154 this haze event (Figure S2).

155

156 3 Results

157 3.1 High potential reduction of wintertime NH_3 emissions in northern China

158 Livestock husbandry accounts for the largest proportion of NH_3 emissions in winter
159 of northern China (approximately 60%), which is mainly caused by the poor manure
160 management. There are three main animal-rearing systems in China: free-range, grazing
161 and intensive. On the one hand, the proportion of intensive livestock husbandry in China



162 is only about 40%, far lower than that of developed countries. As a result, the widespread
163 free-range and grazing animal rearing systems contribute more than half of the total
164 livestock NH_3 emissions due to lacking manure collection and treatment (Kang et al., 2016).
165 On the other hand, there were no relevant regulations about storage and application of
166 manure for intensive farms in China in the past few decades. This causes most livestock
167 farms also lack necessary measures and facilities for manure collection and storage
168 (Chadwick et al., 2015). Meanwhile, most of the solid fraction of manure is applied to
169 crops without any treatment and the liquid fraction is often discharged directly (Bai et al.,
170 2017).

171 Due to the current poor manure management in China, the improved manure
172 management may have great potential for NH_3 emission reductions from livestock
173 husbandry (Wang et al., 2017). The improved manure management mainly includes three
174 phases: in-house handling, storage and land application (Chadwick et al., 2011). According
175 to previous studies, for in-house handling, regularly washing the floor and using slatted
176 floor or deep litter to replace solid floor could both reduce NH_3 emissions by more than 50%
177 (Monteny and Erisman, 1998; Hou et al., 2015). For storage, covering slurry and manure
178 could reduce NH_3 emissions by about 50%-70% (Hou et al., 2015; Wang et al., 2017). For
179 land application, cultivating the soil surface before application or incorporation and
180 injection could both reduce NH_3 emissions by more than 50% (Sommer and Hutchings,
181 2001; Hou et al., 2015).

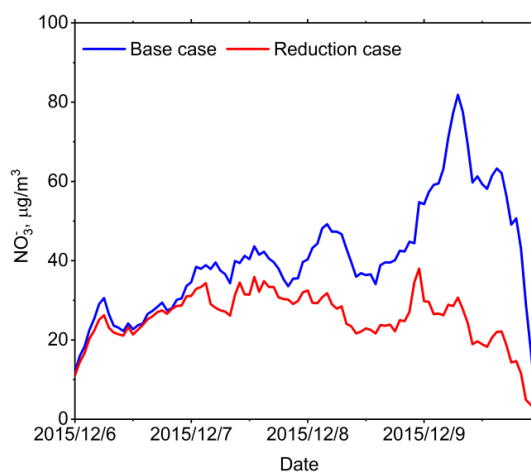
182 Based on the above research results, the livestock NH_3 emission reductions strategies
183 applied in this study include the following steps. Firstly, the proportion of intensive
184 livestock production was raised from 40% to 80% in our NH_3 emission inventory model.
185 In our model, the animals in free-range and grazing animal rearing systems are assumed to
186 live outdoors for half a day, and the improved manure management is only effective for
187 indoor animals. Therefore, increasing the proportion of intensive livestock production is
188 conducive to better manure management (Hristov et al., 2011). Secondly, the ratios of NH_3
189 emission reductions mentioned above were multiplied by NH_3 emission factors in three
190 phases of manure management: 50% reduction at in-house handling, 60% (average value
191 of 50% and 70%) reduction at storage and 50% reduction at land application. With these
192 measures, we estimate that the NH_3 emission factors for the livestock in China could be
193 comparable to those in Europe and the USA (shown in Table S1). Meanwhile, the NH_3
194 emission model predicted that the livestock NH_3 emissions were reduced by 60% (from 57
195 to 23 kiloton), causing approximately 40% reduction in total NH_3 emissions. Spatially,
196 NH_3 emissions decreased significantly in Hebei, Henan and Shandong, where the livestock
197 NH_3 emissions accounted for a large proportion of the total (shown in Figure S3).

198 3.2. Simulations of NO_3^- reduction due to NH_3 emission controls

199 In the ISORROPIA-II simulation, 40% reduction of TA was used to reflect the effects
200 of reducing NH_3 emissions by 40%. In this haze event (from 6 to 10 December, 2015), the
201 mean concentration of particulate NO_3^- decreased from 40.8 to 25.7 $\mu\text{g}/\text{m}^3$ (a 37%
202 reduction). In addition, the peak hourly concentration of NO_3^- decreased from 81.9 to 30.7
203 $\mu\text{g}/\text{m}^3$ (a 63% reduction) (shown in Figure 1). The fundamental thermodynamic processes
204 of TA reductions on decreasing particulate NO_3^- are explained below. Firstly, we found that
205 NH_3 was quite available to react with HNO_3 in the thermodynamic equilibrium system,
206 because NH_3 was $6.6 \pm 3.8 \mu\text{g}/\text{m}^3$ while HNO_3 was only $0.4 \pm 1.1 \mu\text{g}/\text{m}^3$. Secondly, almost
207 all of particulate NO_3^- condensed into aerosol phase (the mass ratio of particulate NO_3^- to



208 TN was $99.2 \pm 1.9\%$) under such low temperature conditions (276.5 ± 1.4 K). Thirdly, the
209 $\text{NH}_3\text{-HNO}_3$ partial pressure production (K_p) was as low as about 0.1 ppb^2 (calculated from
210 ISORROPIA-II outputs, depending not only on temperature and RH but also sulfate
211 concentration). The value of K_p would remain constant, if the temperature, RH and sulfate
212 concentration remained unchanged. In general, NH_4NO_3 was not easy to volatilize into gas
213 phase under these circumstances.



214

215 **Figure 1.** A comparison of particulate nitrate (NO_3^-) between the base (blue line) and
216 emission reductions cases (red line) simulated by the ISORROPIA-II model in this severe
217 haze episode.

218

219 When TA was reduced by 40%, the average mass concentration of gaseous NH_3
220 decreased from 6.6 to $0.01 \text{ } \mu\text{g}/\text{m}^3$ (from 8.8 ppb to 0.05 ppb). In order to keep the value of
221 K_p constant in the thermodynamic equilibrium state, the reductions of NH_3 increased HNO_3 ,
222 which shifted the particulate NO_3^- partitioning toward the gas phase. Hence, when NH_3 in
223 gas phase was almost completely depleted, HNO_3 increased from 0.4 to $15.5 \text{ } \mu\text{g}/\text{m}^3$ (from
224 0.1 ppb to 5.6 ppb), leading to a reduction of particulate NO_3^- from 40.8 to $25.7 \text{ } \mu\text{g}/\text{m}^3$ (a
225 37% reduction). Meanwhile, NH_4^+ also decreased from 27.9 to $20.6 \text{ } \mu\text{g}/\text{m}^3$ and there was
226 almost no change in sulfate level (decreased from 39.7 to $39.3 \text{ } \mu\text{g}/\text{m}^3$), with only trace
227 amount of NH_4HSO_4 produced. This indicated that the reduction of particulate NH_4^+ and
228 NO_3^- was mainly due to the reduction of NH_4NO_3 .

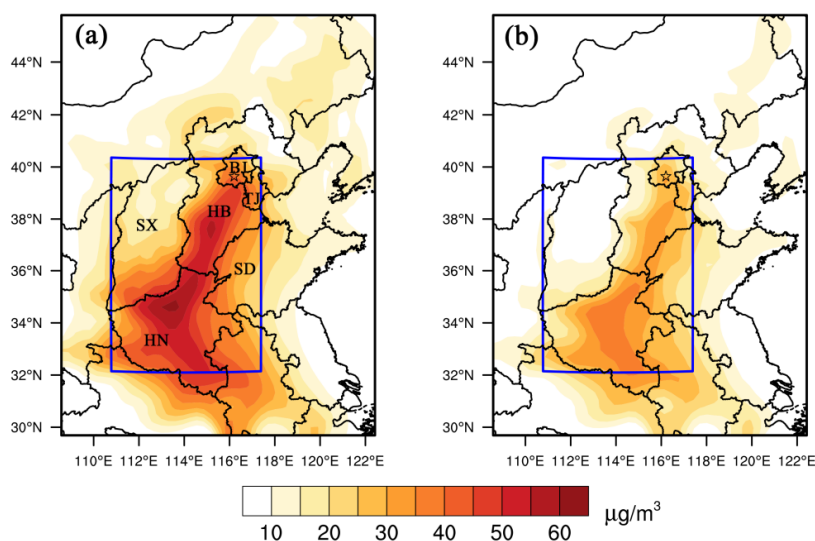
229

230 The above process could also be explained by the interactions between aerosol acidity
231 and gas-particle partitioning of HNO_3 . Guo et al. (2018) used the S curves to demonstrate
232 the relationship between aerosol pH and HNO_3 partitioning in the United States, Europe
233 and China. The results showed that when TA was reduced to a certain extent, aerosol pH
234 began to decline, prompting the particulate NO_3^- volatilizing into gas phase. However,
235 using aerosol pH as an indicator of the sensitivity of particulate NO_3^- to TA has some
236 limitations. On the one hand, it may not be suitable for low temperature or low relative
humidity conditions. Because under these conditions, the estimation of aerosol pH would



237 become inaccurate (Fountoukis et al., 2009). On the other hand, recent studies showed
238 many factors could cause bias in aerosol pH prediction. For instance, Vasilakos et al. (2018)
239 found that non-volatile cations (K^+ , Na^+ , Ca^{2+} and Mg^{2+}) in the fine mode could cause bias
240 in the aerosol pH and HNO_3 partitioning prediction. Silvern et al. (2017) found that
241 particles coated by organic material might retard the uptake of NH_3 , which may also cause
242 bias in modeling aerosol acidity and HNO_3 partitioning. In general, studying the process
243 of aerosol acidity affecting particulate NO_3^- formation still requires more work to do,
244 especially sensitivity tests, to unravel the potential effects of other factors.

245 We also conducted WRF-Chem simulations to quantify the impacts of NH_3 emission
246 controls on particulate NO_3^- regionally. A 60% reduction in livestock NH_3 emissions was
247 used as an emission reductions scheme and Figure 2 shows the spatial distribution of
248 particulate NO_3^- under the base case and the emission reductions case. The spatial
249 distribution of particulate NO_3^- was mainly concentrated in most parts of Henan (HN) and
250 Hebei (HB), with the average concentration over $30 \mu g/m^3$ (included in the blue box shown
251 in Figure 2a). The highest particulate NO_3^- concentrations, more than $60 \mu g/m^3$, were
252 mainly located in central south of Hebei and northern Henan. In the emission reductions
253 case, the mean concentration of particulate NO_3^- decreased from 34.2 to $20.7 \mu g/m^3$ (a 40%
254 reduction) in the range of the blue box. In addition, the sulfate concentration slightly
255 changed from 28.1 to $24.3 \mu g/m^3$, and $PM_{2.5}$ concentration dropped from 161.7 to 139.3
256 $\mu g/m^3$. The largest reductions in particulate NO_3^- were mainly located in the central north
257 of Henan and central Hebei, where the percentage reduction was generally more than 60%
258 (shown in Figure 2b). In these regions, severe haze events occurred frequently due to their
259 large emissions of air pollutants, including NH_3 (Wang et al., 2014; Zhao et al., 2017). The
260 contrast of figure 2a and 2b shows that particulate NO_3^- had been effectively reduced,
261 especially in high concentration areas. The reason is explained in Sect. 3.3.



262

263 **Figure 2. (a)** Spatial distribution of particulate NO_3^- concentrations in northern China
264 predicted by WRF-Chem from 6 to 10 December, 2015, for (a) the base case, and (b) the



265 emission reductions case. The scope of this study focuses on the blue box, including Beijing
266 (BJ), Tianjin (TJ), Hebei (HB), Shanxi (SX), Shangdong (SD) and Henan (HN).

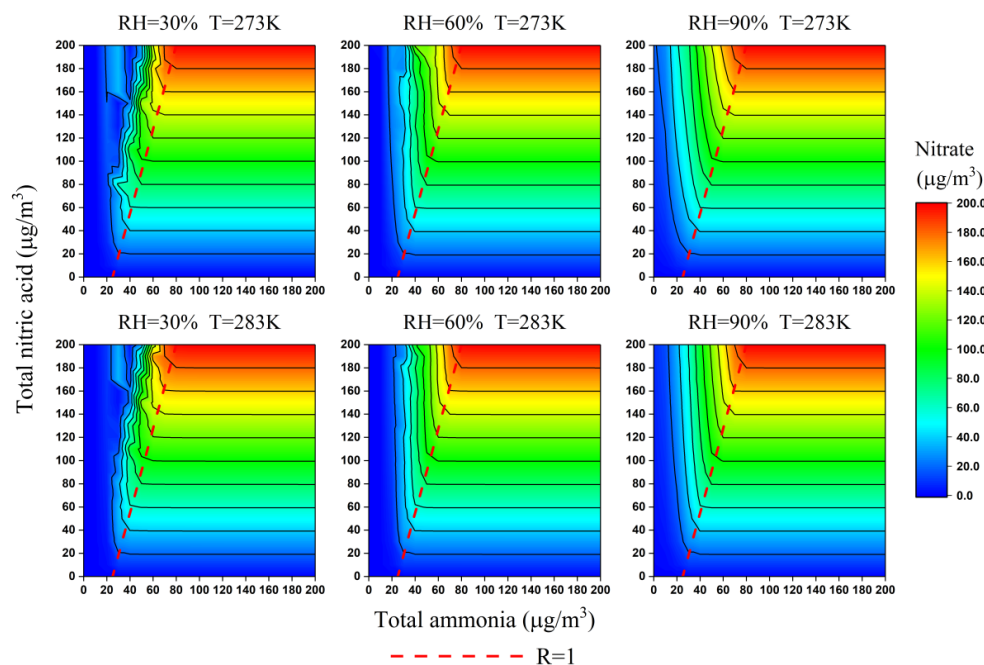
267

268 3.3 The particulate NO₃⁻ reduction efficiency during the wintertime

269 The sensitivity of particulate NO₃⁻ to NH₃ is often determined by the availability of
270 ambient NH₃, which can be represented by the observable indicator (Seinfeld and Pandis,
271 2006). In this study, we use the observed molar ratio (R) of TA to the sum of sulfate, total
272 chlorine and TN minus Na⁺, K⁺, Ca²⁺ and Mg²⁺ to represent the availability of ambient
273 NH₃ and predict the sensitivity of the particulate NO₃⁻ to changes in TN and TA.

$$274 \quad R = \frac{TA}{2SO_4^{2-} + NO_3^- + HNO_3(g) + Cl^- + HCl(g) - 2Ca^{2+} - Na^+ - K^+ - 2Mg^{2+}} \quad (1)$$

275 The accuracy of R was examined by constructing the isopleths of particulate NO₃⁻
276 concentrations as a function of TN and TA (shown in Figure 3). The NO₃⁻ concentration
277 was constructed by varying the input concentrations of TA and TN from 0 to 200 μg/m³
278 in increments of 10 μg/m³ independently in ISORROPIA-II, while using the observed average
279 value for the other components. Over a range of temperatures (273–283 K) and RHs (30–
280 90%), the dashed line of R = 1 divides each isopleth into two regions with tiny bias, which
281 indicates that R can be used to qualitatively predict the response of the particulate NO₃⁻ to
282 changes in concentrations of TN and TA.



283

284 **Figure 3.** Isopleths of the particulate NO₃⁻ concentration (μg/m³) as a function of TN
285 and TA under average severe haze conditions in winter. The concentration of SO₄²⁻, Cl⁻, K⁺,

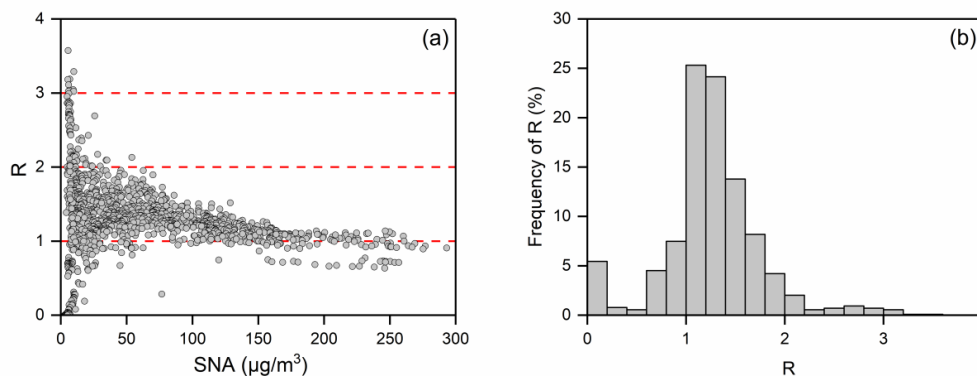


286 Ca^{2+} , Na^+ , and Mg^{2+} was 60.2, 9.3, 0.56, 0.04, 0.75, and 0.03 $\mu\text{g}/\text{m}^3$, respectively. Values
287 are averages from all severe hazes during the observation period.

288

289 In the right side of the dashed line ($R > 1$), particulate NO_3^- formation is HNO_3 -limited.
290 The NH_3 is surplus and almost all particulate NO_3^- exists in the aerosol phase. The TA
291 reductions mainly reduce NH_3 , with negligible effects on particulate NO_3^- . By contrast,
292 particulate NO_3^- formation is NH_3 -limited in the left of the dashed line ($R < 1$). There is
293 less NH_3 present in the gas phase, and TA reductions could reduce particulate NO_3^-
294 efficiently. For example, when the concentrations of TN and TA are 100 and 50 $\mu\text{g}/\text{m}^3$ (RH
295 = 60 % and $T = 273 \text{ K}$), the concentration of particulate NO_3^- is about 100 $\mu\text{g}/\text{m}^3$ and the
296 value of R is close to one (typical observational values during the severe haze in this study).
297 In such cases, if TA were reduced by 50% to 25 $\mu\text{g}/\text{m}^3$, the particulate NO_3^- would be
298 significantly reduced from 100 to 20 $\mu\text{g}/\text{m}^3$, an 80% reduction.

299 Under the typical winter conditions in northern China, the value of R was generally
300 greater than one and gradually declining with the increase in SNA concentrations (shown
301 in Figure 4a). When the concentration of SNA is greater than 150 $\mu\text{g}/\text{m}^3$, the values of R
302 become close to and frequently lower than one. This indicated that particulate NO_3^-
303 formation would easily become NH_3 -limited under severe haze conditions when NH_3
304 emissions were reduced. In general, particulate NO_3^- will be reduced effectively by a 40%
305 reduction of NH_3 emissions in the condition that the value of R is less than 1.4 (shown in
306 Figure S4). This situation accounts for 68.1% of the entire December (shown in Figure 4b).
307 It should also be noted that the particulate NO_3^- can be insensitive to a 40% reduction in
308 NH_3 emissions when the value of R is greater than 1.4 (shown in Figure S4). This situation
309 mainly occurs in relatively clean days (the concentration of SNA is less than 75 $\mu\text{g}/\text{m}^3$),
310 accounting for only 31.9% of the entire December (shown in Figure 4a and 4b). Overall,
311 reducing 40% of NH_3 emissions could effectively reduce the levels of particulate NO_3^-
312 under typical winter haze conditions in northern China.



313

314 **Figure 4.** (a) The observed molar ratio (R) and the concentrations of SNA in PKUERS
315 in December 2015 and December 2016. (b) The frequency of R during the same period.

316

317



318 4 Discussions

319 Improved manure management could reduce 40% of NH₃ emissions in winter of
320 northern China. For a 40% reduction of TA in the atmosphere, ISORROPIA-II predicts that
321 particulate NO₃⁻ could be reduced by 37% for the haze event (from 40.8 to 25.7 μg/m³).
322 When NH₃ emissions are reduced by 40%, the WRF-Chem simulation shows that
323 particulate NO₃⁻ concentration could be reduced effectively throughout the whole region
324 (the mean concentration of particulate NO₃⁻ was reduced from 34.2 to 20.7 μg/m³, a 40%
325 reduction), especially in the area with high particulate NO₃⁻ concentration (more than 60%).
326 The molar ratio (R) of winter observational data in northern China shows that as the
327 concentration of inorganic salts increases, the excess NH₃ in the atmosphere is decreasing,
328 and particulate NO₃⁻ becomes more sensitive to NH₃ emission reductions. In general,
329 controlling livestock NH₃ emissions could be an effective measure to reduce NH₃ levels
330 and limit particulate NO₃⁻ formation.

331 The observed R provides a simple method to rapidly estimate the efficiency of NH₃
332 emission reductions on the particulate NO₃⁻ reductions, which can avoid the shortage of the
333 air quality model, especially the uncertain estimates of meteorology. However, it also has
334 some limitations, such as requiring accurate measurements of water-soluble ions and
335 gaseous components. In addition, the accuracy of R needs to be examined in more detail
336 for specific pollution and meteorological conditions. Therefore, the observed indicator and
337 air quality models should be used in a complementary way to assess the effectiveness of
338 NH₃ emission controls strategies.

339 NO_x emission controls could be a more direct and effective way to reduce the
340 particulate NO₃⁻ than NH₃ emission reductions. However, in northern China, the target of
341 NO_x emission reductions is only about 25% in the 13th Five-Year Plan (2016-2020).
342 Furthermore, the previous study has shown that NO_x emission reductions in the U.S could
343 be much costly to control PM_{2.5} than reductions in NH₃ emission (Pinder et al., 2007). Due
344 to the dominance of extensive livestock farming and the lack of emission controls policies,
345 NH₃ emission reductions in China may be easier and cost less than the U.S. Therefore, in
346 order to control PM_{2.5} pollution more effectively in northern China, NH₃ emission controls
347 are urgently needed. In addition, a comprehensive cost-effectiveness analysis of NH₃
348 emission control strategies in China is also much needed in the future.

349 It should be noted that the NH₃ emission reductions have plenty of significant
350 environmental implications. On the one hand, it could increase the particle acidity to
351 increase the solubility of transition metals in aerosol phase, which is related to aerosol
352 oxidative stress and toxicity (Fang et al., 2017; Longo et al., 2016). Meanwhile, metal
353 mobility could affect photosynthesis productivity (Duce and Tindale, 1991; Li et al., 2017c)
354 and oxygen levels in the ocean (Ito et al., 2016) by changing nutrient distributions.
355 Furthermore, particle strong acidity has also been directly linked to adverse respiratory
356 effects (Schlesinger, 2007; Ward et al., 2002). On the other hand, anthropogenic NH₃
357 emission controls can decrease excess reactive nitrogen inputs to earth ecosystems, which
358 could alleviate many adverse ecological effects including soil acidification, plant
359 biodiversity reduction, and eutrophication (Bouwman et al., 2002; Stevens et al.,
360 2004; Bowman et al., 2008). All these environmental impacts in China require further
361 research.



362 Acknowledgement

363 This study was supported by National Key R&D Program of China (2016YFC0201505)
364 and National Natural Science Foundation of China (NSFC) (91644212, 41675142,
365 21625701 and 41571130033). The data used in this study are available from the
366 corresponding author. The authors declare no competing interests.

367

368 References

369

370 Bai, Z. H., Li, X. X., Lu, J., Wang, X., Velthof, G. L., Chadwick, D., Luo, J. F., Ledgard,
371 S., Wu, Z. G., Jin, S. Q., Oenema, O., Ma, L., and Hu, C. S.: Livestock Housing and
372 Manure Storage Need to Be Improved in China, *Environ. Sci. Technol.*, 51, 8212-
373 8214, 10.1021/acs.est.7b02672, 2017.

374 Bouwman, A. F., Van Vuuren, D. P., Derwent, R. G., and Posch, M.: A global analysis of
375 acidification and eutrophication of terrestrial ecosystems, *Water Air Soil Pollut.*, 141,
376 349-382, Doi 10.1023/A:1021398008726, 2002.

377 Bowman, W. D., Cleveland, C. C., Halada, L., Hresko, J., and Baron, J. S.: Negative impact
378 of nitrogen deposition on soil buffering capacity, *Nat. Geosci.*, 1, 767-770,
379 10.1038/ngeo339, 2008.

380 Chadwick, D., Sommer, S. G., Thorman, R., Fanguero, D., Cardenas, L., Amon, B., and
381 Misselbrook, T.: Manure management: Implications for greenhouse gas emissions,
382 *Anim Feed Sci Tech*, 166-67, 514-531, 10.1016/j.anifeedsci.2011.04.036, 2011.

383 Chadwick, D., Jia, W., Tong, Y. A., Yu, G. H., Shen, Q. R., and Chen, Q.: Improving
384 manure nutrient management towards sustainable agricultural intensification in China,
385 *Agr Ecosyst Environ*, 209, 34-46, 10.1016/j.agee.2015.03.025, 2015.

386 Duce, R. A., and Tindale, N. W.: Atmospheric Transport of Iron and Its Deposition in the
387 Ocean, *Limnol. Oceanogr.*, 36, 1715-1726, DOI 10.4319/lo.1991.36.8.1715, 1991.

388 Elser, M., Huang, R. J., Wolf, R., Slowik, J. G., Wang, Q. Y., Canonaco, F., Li, G. H.,
389 Bozzetti, C., Daellenbach, K. R., Huang, Y., Zhang, R. J., Li, Z. Q., Cao, J. J.,
390 Baltensperger, U., El-Haddad, I., and Prevot, A. S. H.: New insights into PM_{2.5}
391 chemical composition and sources in two major cities in China during extreme haze
392 events using aerosol mass spectrometry, *Atmos. Chem. Phys.*, 16, 3207-3225,
393 10.5194/acp-16-3207-2016, 2016.

394 Fang, T., Guo, H. Y., Zeng, L. H., Verma, V., Nenes, A., and Weber, R. J.: Highly Acidic
395 Ambient Particles, Soluble Metals, and Oxidative Potential: A Link between Sulfate
396 and Aerosol Toxicity, *Environ. Sci. Technol.*, 51, 2611-2620,
397 10.1021/acs.est.6b06151, 2017.

398 Fast, J. D., Gustafson, W. I., Easter, R. C., Zaveri, R. A., Barnard, J. C., Chapman, E. G.,
399 Grell, G. A., and Peckham, S. E.: Evolution of ozone, particulates, and aerosol direct
400 radiative forcing in the vicinity of Houston using a fully coupled meteorology-
401 chemistry-aerosol model, *J. Geophys. Res.-Atmos.*, 111, 10.1029/2005jd006721,
402 2006.

403 Fountoukis, C., and Nenes, A.: ISORROPIA II: a computationally efficient
404 thermodynamic equilibrium model for K⁺-Ca²⁺-Mg²⁺-NH₄⁺-Na⁺-SO₄²⁻-NO₃⁻-Cl⁻
405 -H₂O aerosols, *Atmos. Chem. Phys.*, 7, 4639-4659, 10.5194/acp-7-4639-2007, 2007.

406 Fountoukis, C., Nenes, A., Sullivan, A., Weber, R., Van Reken, T., Fischer, M., Matias, E.,
407 Moya, M., Farmer, D., and Cohen, R. C.: Thermodynamic characterization of Mexico



- 408 City aerosol during MILAGRO 2006, *Atmos Chem Phys*, 9, 2141-2156, 10.5194/acp-
409 9-2141-2009, 2009.
- 410 Fu, X., Wang, S. X., Xing, J., Zhang, X. Y., Wang, T., and Hao, J. M.: Increasing Ammonia
411 Concentrations Reduce the Effectiveness of Particle Pollution Control Achieved via
412 SO₂ and NO_x Emissions Reduction in East China, *Environ. Sci. Technol. Lett.*, 4,
413 221-227, 10.1021/acs.estlett.7b00143, 2017.
- 414 Geng, G., Zhang, Q., Tong, D., Li, M., Zheng, Y., Wang, S., and He, K.: Chemical
415 composition of ambient PM_{2.5} over China and relationship to precursor emissions
416 during 2005–2012, *Atmos. Chem. Phys.*, 17, 9187-9203, 10.5194/acp-17-9187-2017,
417 2017.
- 418 Guo, H., Otjes, R., Schlag, P., Kiendler-Scharr, A., Nenes, A., and Weber, R. J.:
419 Effectiveness of Ammonia Reduction on Control of Fine Particle Nitrate,
420 *Atmospheric Chemistry and Physics Discussions*, 1-31, 10.5194/acp-2018-378, 2018.
- 421 Hou, Y., Velthof, G. L., and Oenema, O.: Mitigation of ammonia, nitrous oxide and
422 methane emissions from manure management chains: a meta-analysis and integrated
423 assessment, *Glob. Change Biol.*, 21, 1293-1312, 2015.
- 424 Hristov, A. N., Hanigan, M., Cole, A., Todd, R., McAllister, T. A., Ndegwa, P. M., and
425 Rotz, A.: Review: Ammonia emissions from dairy farms and beef feedlots, *Can J*
426 *Anim Sci*, 91, 1-35, 2011.
- 427 Huang, R. J., Zhang, Y., Bozzetti, C., Ho, K. F., Cao, J. J., Han, Y., Daellenbach, K. R.,
428 Slowik, J. G., Platt, S. M., Canonaco, F., Zotter, P., Wolf, R., Pieber, S. M., Bruns, E.
429 A., Crippa, M., Ciarelli, G., Piazzalunga, A., Schwikowski, M., Abbaszade, G.,
430 Schnelle-Kreis, J., Zimmermann, R., An, Z., Szidat, S., Baltensperger, U., El Haddad,
431 I., and Prevot, A. S.: High secondary aerosol contribution to particulate pollution
432 during haze events in China, *Nature*, 514, 218-222, 10.1038/nature13774, 2014.
- 433 Huang, X., Song, Y., Li, M. M., Li, J. F., Huo, Q., Cai, X. H., Zhu, T., Hu, M., and Zhang,
434 H. S.: A high-resolution ammonia emission inventory in China, *Glob. Biogeochem.*
435 *Cycle*, 26, 10.1029/2011gb004161, 2012.
- 436 Ito, T., Nenes, A., Johnson, M. S., Meskhidze, N., and Deutsch, C.: Acceleration of oxygen
437 decline in the tropical Pacific over the past decades by aerosol pollutants, *Nat. Geosci.*,
438 9, 443-+, 10.1038/Ngeo2717, 2016.
- 439 Kang, Y. N., Liu, M. X., Song, Y., Huang, X., Yao, H., Cai, X. H., Zhang, H. S., Kang, L.,
440 Liu, X. J., Yan, X. Y., He, H., Zhang, Q., Shao, M., and Zhu, T.: High-resolution
441 ammonia emissions inventories in China from 1980 to 2012, *Atmos. Chem. Phys.*, 16,
442 2043-2058, 10.5194/acp-16-2043-2016, 2016.
- 443 Li, C., McLinden, C., Fioletov, V., Krotkov, N., Carn, S., Joiner, J., Streets, D., He, H.,
444 Ren, X., Li, Z., and Dickerson, R. R.: India Is Overtaking China as the World's Largest
445 Emitter of Anthropogenic Sulfur Dioxide, *Sci Rep*, 7, 14304, 10.1038/s41598-017-
446 14639-8, 2017a.
- 447 Li, H. Y., Zhang, Q., Zhang, Q., Chen, C. R., Wang, L. T., Wei, Z., Zhou, S., Parworth, C.,
448 Zheng, B., Canonaco, F., Prevot, A. S. H., Chen, P., Zhang, H. L., Wallington, T. J.,
449 and He, K. B.: Wintertime aerosol chemistry and haze evolution in an extremely
450 polluted city of the North China Plain: significant contribution from coal and biomass
451 combustion, *Atmos. Chem. Phys.*, 17, 4751-4768, 10.5194/acp-17-4751-2017, 2017b.
- 452 Li, W. J., Xu, L., Liu, X. H., Zhang, J. C., Lin, Y. T., Yao, X. H., Gao, H. W., Zhang, D.
453 Z., Chen, J. M., Wang, W. X., Harrison, R. M., Zhang, X. Y., Shao, L. Y., Fu, P. Q.,



- 454 Nenes, A., and Shi, Z. B.: Air pollution-aerosol interactions produce more
455 bioavailable iron for ocean ecosystems, *Sci Adv*, 3, ARTN e1601749
456 10.1126/sciadv.1601749, 2017c.
- 457 Li, Y. J., Sun, Y., Zhang, Q., Li, X., Li, M., Zhou, Z., and Chan, C. K.: Real-time chemical
458 characterization of atmospheric particulate matter in China: A review, *Atmos.*
459 *Environ.*, 158, 270-304, 10.1016/j.atmosenv.2017.02.027, 2017d.
- 460 Liu, F., Beirle, S., Zhang, Q., van der, A. R., Zheng, B., Tong, D., and He, K.: NO_x
461 emission trends over Chinese cities estimated from OMI observations during 2005 to
462 2015, *Atmos Chem Phys*, 17, 9261-9275, 10.5194/acp-17-9261-2017, 2017a.
- 463 Liu, M. X., Song, Y., Zhou, T., Xu, Z. Y., Yan, C. Q., Zheng, M., Wu, Z. J., Hu, M., Wu,
464 Y. S., and Zhu, T.: Fine particle pH during severe haze episodes in northern China,
465 *Geophys. Res. Lett.*, 44, 5213-5221, 10.1002/2017gl073210, 2017b.
- 466 Longo, A. F., Feng, Y., Lai, B., Landing, W. M., Shelley, R. U., Nenes, A., Mihalopoulos,
467 N., Violaki, K., and Ingall, E. D.: Influence of Atmospheric Processes on the
468 Solubility and Composition of Iron in Saharan Dust, *Environ. Sci. Technol.*, 50, 6912-
469 6920, 10.1021/acs.est.6b02605, 2016.
- 470 Monteny, G. J., and Erisman, J. W.: Ammonia emission from dairy cow buildings: A
471 review of measurement techniques, influencing factors and possibilities for reduction,
472 *Neth J Agr Sci*, 46, 225-247, 1998.
- 473 Pandis, S. N., and Seinfeld, J. H.: On the Interaction between Equilibration Processes and
474 Wet or Dry Deposition, *Atmos Environ a-Gen*, 24, 2313-2327, 10.1016/0960-
475 1686(90)90325-H, 1990.
- 476 Paulot, F., Jacob, D. J., Pinder, R. W., Bash, J. O., Travis, K., and Henze, D. K.: Ammonia
477 emissions in the United States, European Union, and China derived by high-resolution
478 inversion of ammonium wet deposition data: Interpretation with a new agricultural
479 emissions inventory (MASAGE_NH₃), *J. Geophys. Res.-Atmos.*, 119, 4343-4364,
480 10.1002/2013jd021130, 2014.
- 481 Pinder, R. W., Adams, P. J., and Pandis, S. N.: Ammonia emission controls as a cost-
482 effective strategy for reducing atmospheric particulate matter in the eastern United
483 States, *Environ. Sci. Technol.*, 41, 380-386, 10.1021/es060379a, 2007.
- 484 Schlesinger, R. B.: The health impact of common inorganic components of fine particulate
485 matter (PM_{2.5}) in ambient air: A critical review, *Inhal Toxicol*, 19, 811-832,
486 10.1080/08958370701402382, 2007.
- 487 Seinfeld, J. H., and Pandis, S. N.: *Atmospheric chemistry and physics : from air pollution*
488 *to climate change*, 2nd ed., Wiley, New York, xxviii, 1202 p. pp., 2006.
- 489 Silvern, R. F., Jacob, D. J., Kim, P. S., Marais, E. A., Turner, J. R., Campuzano-Jost, P.,
490 and Jimenez, J. L.: Inconsistency of ammonium-sulfate aerosol ratios with
491 thermodynamic models in the eastern US: a possible role of organic aerosol, *Atmos.*
492 *Chem. Phys.*, 17, 5107-5118, 10.5194/acp-17-5107-2017, 2017.
- 493 Sommer, S. G., and Hutchings, N. J.: Ammonia emission from field applied manure and
494 its reduction - invited paper, *Eur J Agron*, 15, 1-15, 2001.
- 495 Stevens, C. J., Dise, N. B., Mountford, J. O., and Gowing, D. J.: Impact of nitrogen
496 deposition on the species richness of grasslands, *Science*, 303, 1876-1879, DOI
497 10.1126/science.1094678, 2004.
- 498 Van Damme, M., Clarisse, L., Heald, C. L., Hurtmans, D., Ngadi, Y., Clerbaux, C., Dolman,
499 A. J., Erisman, J. W., and Coheur, P. F.: Global distributions, time series and error



- 500 characterization of atmospheric ammonia (NH₃) from IASI satellite observations,
501 Atmos. Chem. Phys., 14, 2905-2922, 10.5194/acp-14-2905-2014, 2014.
- 502 Vasilakos, P., Russell, A., Weber, R., and Nenes, A.: Understanding nitrate formation in a
503 world with less sulfate, Atmospheric Chemistry and Physics Discussions, 1-27,
504 10.5194/acp-2018-406, 2018.
- 505 Wang, L. T., Wei, Z., Yang, J., Zhang, Y., Zhang, F. F., Su, J., Meng, C. C., and Zhang,
506 Q.: The 2013 severe haze over southern Hebei, China: model evaluation, source
507 apportionment, and policy implications, Atmos. Chem. Phys., 14, 3151-3173,
508 10.5194/acp-14-3151-2014, 2014.
- 509 Wang, Y., Zhang, Q. Q., He, K., Zhang, Q., and Chai, L.: Sulfate-nitrate-ammonium
510 aerosols over China: response to 2000-2015 emission changes of sulfur dioxide,
511 nitrogen oxides, and ammonia, Atmos. Chem. Phys., 13, 2635-2652, 10.5194/acp-13-
512 2635-2013, 2013.
- 513 Wang, Y., Dong, H. M., Zhu, Z. P., Gerber, P. J., Xin, H. W., Smith, P., Opio, C., Steinfeld,
514 H., and Chadwick, D.: Mitigating Greenhouse Gas and Ammonia Emissions from
515 Swine Manure Management: A System Analysis, Environ. Sci. Technol., 51, 4503-
516 4511, 2017.
- 517 Wang, Y. H., Liu, Z. R., Zhang, J. K., Hu, B., Ji, D. S., Yu, Y. C., and Wang, Y. S.: Aerosol
518 physicochemical properties and implications for visibility during an intense haze
519 episode during winter in Beijing, Atmos. Chem. Phys., 15, 3205-3215, 10.5194/acp-
520 15-3205-2015, 2015.
- 521 Ward, D. J., Roberts, K. T., Jones, N., Harrison, R. M., Ayres, J. G., Hussain, S., and
522 Walters, S.: Effects of daily variation in outdoor particulates and ambient acid species
523 in normal and asthmatic children, Thorax, 57, 489-502, DOI 10.1136/thorax.57.6.489,
524 2002.
- 525 Yang, T., Sun, Y., Zhang, W., Wang, Z., Liu, X., Fu, P., and Wang, X.: Evolutionary
526 processes and sources of high-nitrate haze episodes over Beijing, Spring, J Environ
527 Sci-China, 54, 142-151, 10.1016/j.jes.2016.04.024, 2017.
- 528 Yang, Y. R., Liu, X. G., Qu, Y., An, J. L., Jiang, R., Zhang, Y. H., Sun, Y. L., Wu, Z. J.,
529 Zhang, F., Xu, W. Q., and Ma, Q. X.: Characteristics and formation mechanism of
530 continuous hazes in China: a case study during the autumn of 2014 in the North China
531 Plain, Atmos. Chem. Phys., 15, 8165-8178, 10.5194/acp-15-8165-2015, 2015.
- 532 Zaveri, R. A., Easter, R. C., and Peters, L. K.: A computationally efficient multicomponent
533 equilibrium solver for aerosols (MESA), J. Geophys. Res.-Atmos., 110,
534 10.1029/2004jd005618, 2005.
- 535 Zaveri, R. A., Easter, R. C., Fast, J. D., and Peters, L. K.: Model for Simulating Aerosol
536 Interactions and Chemistry (MOSAIC), J. Geophys. Res.-Atmos., 113,
537 10.1029/2007jd008782, 2008.
- 538 Zhang, L., Chen, Y. F., Zhao, Y. H., Henze, D. K., Zhu, L. Y., Song, Y., Paulot, F., Liu,
539 X. J., Pan, Y. P., Lin, Y., and Huang, B. X.: Agricultural ammonia emissions in China:
540 reconciling bottom-up and top-down estimates, Atmos. Chem. Phys., 18, 339-355,
541 10.5194/acp-18-339-2018, 2018.
- 542 Zhang, X. Y., Wang, J. Z., Wang, Y. Q., Liu, H. L., Sun, J. Y., and Zhang, Y. M.: Changes
543 in chemical components of aerosol particles in different haze regions in China from
544 2006 to 2013 and contribution of meteorological factors the, Atmos. Chem. Phys., 15,
545 12935-12952, 10.5194/acp-15-12935-2015, 2015.



-
- 546 Zhao, B., Wu, W. J., Wang, S. X., Xing, J., Chang, X., Liou, K. N., Jiang, J. H., Gu, Y.,
547 Jang, C., Fu, J. S., Zhu, Y., Wang, J. D., Lin, Y., and Hao, J. M.: A modeling study of
548 the nonlinear response of fine particles to air pollutant emissions in the Beijing-
549 Tianjin-Hebei region, *Atmos. Chem. Phys.*, 17, 12031-12050, 10.5194/acp-17-12031-
550 2017, 2017.
- 551 Zheng, G. J., Duan, F. K., Su, H., Ma, Y. L., Cheng, Y., Zheng, B., Zhang, Q., Huang, T.,
552 Kimoto, T., Chang, D., Poschl, U., Cheng, Y. F., and He, K. B.: Exploring the severe
553 winter haze in Beijing: the impact of synoptic weather, regional transport and
554 heterogeneous reactions, *Atmos. Chem. Phys.*, 15, 2969-2983, 10.5194/acp-15-2969-
555 2015, 2015.
- 556
557
558
559
560
561